Electroencephalography and clinical Neurophysiology, 90 (1994) 229–241

EEG 92726

A multiple source approach to the correction of eye artifacts

Patrick Berg [a,*] and Michael Scherg [b]

[a] *Dept. of Psychology, University of Konstanz, Postfach 5560, 78434 Konstanz (FRG), and*
[b] *Dept. of Neurology, University of Heidelberg, Heidelberg (FRG)*

(Accepted for publication: 17 September 1993)

Summary Previously published methods correct eye artifacts by subtracting proportions of the EOG from EEG electrodes. The implicit assumption made by these methods is that the EOG signals are a good measure of eye activity and contain no EEG. In this paper a new *multiple source eye correction* (MSEC) method of eye artifact treatment based on multiple source analysis is presented, which incorporates a model of brain activity. An accurate, head model-independent estimate of the spatial distribution of eye activity can be obtained empirically from calibration data containing systematic eye movements and blinks. Using the resulting spatial vectors together with the brain model, eye activity in EEG and event-related response data can be estimated in the presence of overlapping brain activity and corrected. A consequence of the MSEC approach is that data at EOG electrodes can be included in analyses of brain activity. In addition, by suitable selection of the spatial vectors, the eye activity can be split into signals which identify vertical and horizontal movements and eyeblinks.

Using auditory ERP data sets with and without large eye artifacts, the MSEC method is compared with a "traditional" method in which brain activity is not modelled, particularly with respect to the spatial distribution of the corrected EEG. Traditional eye correction methods are shown to alter the spatial distribution of the EEG, resulting, for example, in changes in location and orientation of modelled equivalent sources. Such distortion is much reduced in the MSEC method, thus enhancing the precision of topographical EEG analyses.

Key words: EOG; Eye movements; Eye artifact correction; Dipole sources; Multiple sources; EEG

The basic assumption underlying eye artifact correction methods is that the measured EEG consists of the sum of the "real" EEG and eye movement-induced artifacts. In previously published correction methods (e.g., Gratton et al. 1983; Elbert et al. 1985; Brunia et al. 1989), it has been assumed that the EOG is a "true" measure of the eye activity. *Transmission coefficients* — amplitude relationships between one or more EOG channels and each EEG channel — are estimated, for example using regression. Correction consists of subtracting the estimated proportion of the EOG from the EEG. However, subtracting the EOG from EEG channels subtracts a proportion of brain activity, thus resulting in a change in the topography of the EEG.

It should be possible to improve on correction of eye artifacts if a better estimate could be made of the eye activity without contamination by brain activity. One approach to reduce contamination is to estimate the overlapping contributions of eye and brain activities by modelling the brain activity in the presence of eye movements. In a recent study (Berg and Scherg 1990, 1991a), eye movements and blinks were successfully modelled using equivalent dipoles. However, such models may be inaccurate near the eyes, due to deviations from the spherical head model. This paper describes a new approach, which we call the *multiple source eye correction* (MSEC) method, using empirical measurements to obtain an estimate of the spatial topography due to eye activity that is more accurate than dipole models. The method is compared to a "traditional" method of EOG subtraction which does not incorporate modelling of brain activity. The method has been summarized in Berg and Scherg (1991b) and in Lins et al. (1993), who compare the MSEC method with traditional subtraction methods in its ability to remove eye artifacts.

In this paper we present a full description of the MSEC method and its application to ERP data. We also present an important additional application of the method, i.e., its ability to *identify* different types of eye activity. For example, an EEG record can be generated consisting of the artifact-corrected EEG together with

* Corresponding author. Tel.: (49) 7531 977289; Fax: (49) 7531 977492.

SSDI 0013-4694(93)E0250-A

channels representing vertical and horizontal eye movements and blinks.

The paper is divided into 3 sections. In the first, the MSEC method is described, including the mathematics and information about its practical application. In the second, an example is given showing its use to identify eye activity. In Section III, the method is compared with the traditional approach in its effects on the topography and modelling of auditory N100 data.

(I) The multiple source method of eye artifact correction

Principles of the method

In the MSEC method, empirically determined components are defined that describe the topography of eye activity. They are treated equivalently to dipole sources which model the brain activity within a head model. Both the eye components and the dipole sources are considered as concurrent overlapping processes which may be distinguished and separated by their topography. With this concept, we recognize that *all* channels contain information, in differing proportions, about both eye *and* brain activity.

Thus, the emphasis is changed away from the description of the relationship *between* EOG and EEG channels (used in the traditional methods) to the relationship *among all* channels. Instead of using the term "transmission coefficients" for the eye activity, we define "source vectors" which describe topographic distributions, i.e., relative amplitudes at each electrode, due to some source process. Source vectors describe eye and brain activity in similar ways. They differ only in how they are estimated. The eye source vectors can be measured empirically, e.g., by estimating "transmission coefficients" during voluntary eye movements using regression between EOG and EEG. The brain source vectors can be approximated by the forward coefficients of equivalent dipoles within a head model.

An important aspect of source modelling is the separation of the data into topographic and time-varying parts. We define a "source component" to consist of the combination of these two parts, the topography defined by the source vector and the temporal part defined by the "source wave form." The source wave form is an amplitude function, defining the magnitude of a source component over time. Our task is to establish a spatio-temporal model consisting of source components with specific topographies and source activity wave forms that overlap at the scalp. This model should provide the best fit to the measured data, and at the same time, separate eye and brain activities to the largest possible extent.

Three important consequences follow: (a) eye artifact correction is performed by subtracting the source wave forms rather than the EOG signals from the data, in proportions defined by the relative strength of the source component at each electrode; (b) with appropriate rotation of the components, the source wave forms can also be used to describe the time course of specific eye activities; (c) due to the equal treatment of all electrodes in the MSEC method, after removal of eye artifacts, the EOG electrodes can in principle continue to be used for EEG analysis.

Mathematical principles underlying the method

The mathematics underlying the modelling of the EEG or event-related potentials (ERPs) in terms of multiple overlapping sources have been described elsewhere (e.g., Scherg and Von Cramon 1985; Achim et al. 1988; De Munck 1988; Baumgartner et al. 1989; Scherg 1990; Scherg and Picton 1991). Although the method is described in terms of EEG, the principles are equally applicable to MEG and to other sources of artifact, such as ECG.

The electrical potential $u_k(t)$ at electrode k and time t is assumed to be the linear sum of the contributions (source components) from all the brain, eye and other (muscle, noise) sources:

$$u_k(t) = \sum_{i=1}^{NS} \mathbf{c}_{ki} s_i(t) \qquad (1)$$

where $\mathbf{c}_{ki}$ is the source vector, giving the relative contribution of source i at electrode k (i.e., describes the topography of source i), and $s_i(t)$ is the source wave form describing the amplitude of source i at time t (i.e., the time-varying part). NS is the number of sources.

For a given dipole source model of the electrical potential, the source vectors $\mathbf{c}_{ki}$ are a function of the locations and orientations of each source, and of the head parameters, i.e., the geometry and conductivity properties of the brain, cerebrospinal fluid, skull and scalp. Using linear optimization methods (e.g., the Moore-Penrose pseudoinverse) Eqn. (1) can be solved to obtain the source wave form $s_i(t)$ that results in the best fit of the model to the data, provided that the number of sources does not exceed the number of electrodes. The sum of squares over electrodes of the difference between the measured and predicted potential is expressed as a percentage of the total data variance, the residual variance. The smaller the residual variance, the better the fit of model and data.

To incorporate an eye correction method, sources due to the eyes and the brain are distinguished by splitting the right hand term in Eqn. (1) into two:

$$u_k(t) = \sum_{i=1}^{NB} \mathbf{c}_{ki} s_i(t) + \sum_{j=1}^{NE} \mathbf{e}_{kj} o_j(t) \qquad (2)$$

where $\mathbf{c}_{ki}$ describes the brain source vectors, modelled by dipoles, and $\mathbf{e}_{kj}$ the eye source vectors, determined,

for example by empirical calibration. $s_j(t)$ and $o_i(t)$ are the corresponding source wave forms. The total number of sources (NS) is the combination of NB brain and NE eye sources.

$$NS = NB + NE \quad (3)$$

Note that the right hand element of Eqn. (2) describes eye activity *in the presence of brain activity*. This is the main distinction between the MSEC method and previous eye artifact correction methods. Once the equation has been solved, eye artifact correction can be performed by subtracting the right hand element of Eqn. (2) from the data:

$$w_k(t) = u_k(t) - \sum_{j=1}^{NE} e_{kj} o_j(t) \quad (4)$$

where $w_k(t)$ are the corrected wave forms.

Note that the method incorporates the following 2 assumptions: (1) an adequate number of components (NE) are used to describe eye activity (equivalent to the question about how many EOG channels to use in the traditional methods), and (2) a reasonable model is used to describe the brain activity. These questions are considered in the following two sections.

How to generate eye source vectors

The first requirement for accurate determination of source vectors is a set of data containing eye movements that are sufficiently large to be able to distinguish the vectors from the background (e.g., EEG). This is best achieved using calibration movements, although if only eye blinks are to be corrected, the measurement data can be used. An example of a calibration procedure is given in Section III.

In common with the traditional methods, a sufficient number of eye source vectors needs to be included to describe the different types of eye activity. There are several ways to extract source vectors from the calibration data: we have used transmission coefficients between the EOG and the EEG in part of the empirical evaluation of the MSEC method (Section III) in order to make it more comparable to a traditional method using the same coefficients. A second, more general approach is to apply a principal components analysis (PCA). The PCA can be applied using covariances over all time points of a calibration data set or over averaged eye movements. The PCA generates orthogonal vectors, each constituting a different topography. Some vectors will be due to eye movements, and some due to EEG and noise. Provided that the calibration movements are sufficiently large, we find that the 3 vectors explaining the largest data variance describe only (and most of the) eye activity. With very clean calibration data (Lins et al. 1993), more than 3 vectors may be used. One way to summarize the topography of the components is to compute the centre of gravity of the location and orientation (Scherg and Von Cramon 1984). This is illustrated at the top of Fig. 3. Centres of gravity of components due to eye activity should be located near the eyes.

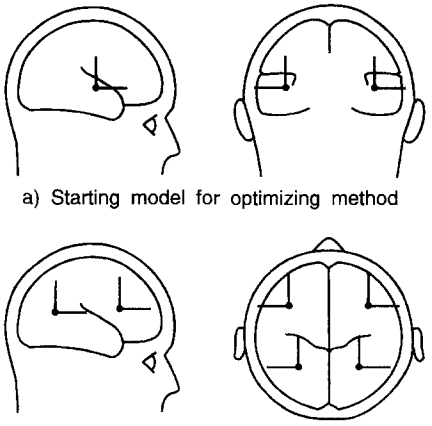

Fig. 1. a: 2 regional sources used as the starting model for fitting the auditory N100 in the optimizing MSEC method and to model each of the uncorrected and corrected data sets. The sources were constrained to be symmetrical in each hemisphere. b: 4 regional sources used to model the EEG in the surrogate MSEC method. Each regional source is described in terms of 3 orthogonal sources at the same location. Source locations are indicated by black circles, orientations by the line emerging from each circle.

How to model brain activity

Two methods of modelling brain activity were tested (Fig. 1). In the first, *optimizing*, method dipole sources were fitted to the data using an iterative technique (cf., Scherg 1990) to optimize the brain activity model in the presence of the (overlapping) eye source components. Such a method is applicable in situations where enough prior knowledge is available to perform such modelling. In general this is possible with ERPs and large EEG signals, for example epileptiform spikes (Ebersole 1991). In the data set analysed in Section III, the N100 time range of auditory ERPs was examined. It is known that the generators of the auditory potential in this time range are mainly in the temporal lobes (Scherg and Von Cramon 1985; Scherg et al. 1989). Fig. 1a shows the starting model applied to the data set, which was optimized for the grand mean and for each individual subject. The model consists of a pair of regional sources (Scherg and Von Cramon 1986), constrained to be symmetrically located in each hemisphere. "Optimization" in the current context consisted of fitting the (symmetrical) location of these sources in the time range between 60 and 200 msec after stimulus onset.

The second, *surrogate* method can be applied in principle to any EEG or averaged data, but it is to be expected that the modelling is less accurate than the optimizing model. The surrogate model consists of a

set of dipole sources placed in the head that are not necessarily at the locations of the EEG generators, but are sufficiently well distributed to be able to "describe" some or most of the EEG. Note that even if only some of the EEG at eye electrodes is modelled, the surrogate MSEC method should produce better results than traditional methods. Some consideration is necessary as to the number of sources to put into the surrogate model. One important factor is the relationship between the total number of sources (brain model plus eye source components) and the number of electrodes. As the number of sources approaches the number of electrodes the solution to Eqn. (2) becomes increasingly arbitrary because noise in the data is enhanced. In our 32-channel data set the 12-source surrogate model (total no. of sources including ocular source components = 15) shown in Fig. 1b was found to result in better eye artifact correction than a 21-source model (total = 24). Only the results of the use of the 12-source model are presented below.

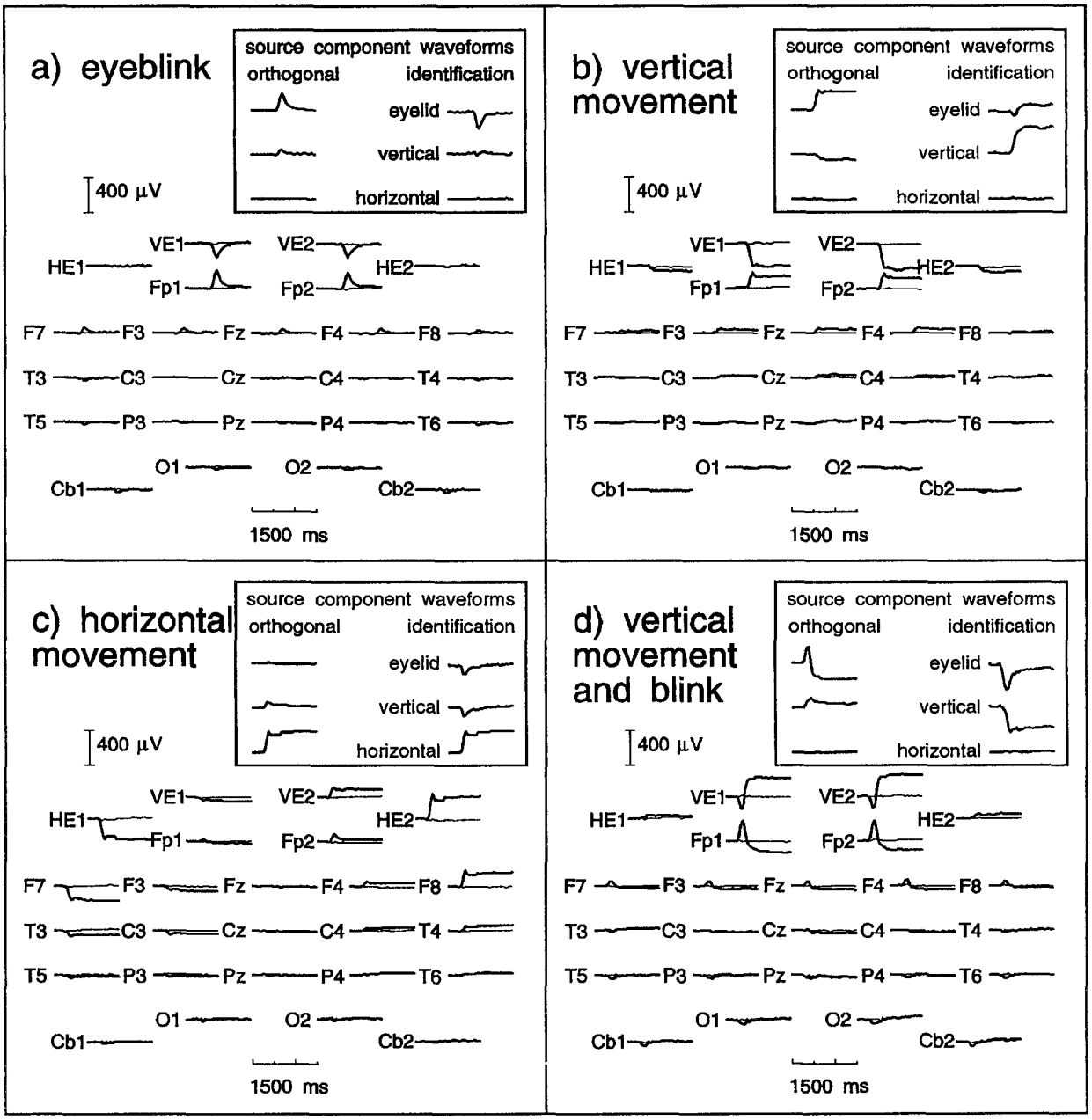

Fig. 2. Average referenced data from four 1500 msec raw EEG epochs from 1 subject, before (thick lines) and after (thin lines) correction using 3 source components and the surrogate EEG model shown in Fig. 1b. Each epoch shows a different type of eye activity: (a) an eyeblink, (b) a vertical movement, (c) a horizontal movement, and (d) an eyeblink overlapping a vertical movement. The source wave forms of the (orthogonal) components used for correction are shown at the top left. At the top right are the source wave forms of the components used for identification. These are able to identify the time course of each type of eye activity, even when they overlap (d). Only 25 of the 33 data channels are shown.

(II) An example of correction of raw data and identification of eye movements using the MSEC method

Fig. 2 shows the results of correcting 4 short (1500 msec) stretches of raw data using the surrogate brain activity model, filtered above 15 Hz (12 dB/octave). The data are selected from the eye calibration movements of a participant of the experiment described in Section III. Two alternative methods were used to compute the eye source vectors. The source wave forms resulting from each method are shown at the top of each subfigure. In the first method, 3 source vectors explaining approximately 95% of the data variance in the PCA were extracted from the combined calibration data from vertical and horizontal eye movements and blinks (top left of each subfigure). In the second method, a PCA was applied separately to an average of each of the 3 types of calibrated eye activity (top right of each subfigure), and the first vector of each PCA was used. In the second method, the vectors individually describe the main variance in each type of eye activity. Therefore the source wave forms in the second method are able to distinguish and identify the overlapping types of eye movement, whereas in the first method the wave forms describe the data in terms of arbitrary combinations of eye activity.

In Fig. 2a–c, wave forms for an eyeblink, a vertical eye movement, and a horizontal eye movement are shown. Each identification wave form should represent one type of eye activity. However, in each of the examples, the wave forms suggest that more than one type of activity occurred. During the blink (Fig. 2a), the vertical movement identification wave form suggests that there was a slight downward and then upward rotation of the eyeball due to the friction of the eyelid. During the vertical upward eye movement there was some activity on the eyeblink wave form (Fig. 2b). This is consistent with the upward eyelid motion accompanying a typical vertical movement.

During the horizontal (rightward) eye movement (Fig. 2c), there was some activity on both vertical and eyeblink wave forms. The small peak at the end of the saccade, visible in particular at electrodes Fp1 and Fp2, appears to correspond to this activity, which was observed in every horizontal movement in this subject. The activity could be due to small eyelid movements associated with horizontal saccades (Billings 1989; Lins et al. 1993), although the activity on the vertical identification wave form suggests that this is not a complete explanation. This example suggests that a single factor is not sufficient to describe the complete topography of horizontal eye movements. A second factor is present, which is described here in terms of the combined activity of the vertical and eyeblink components.

In Fig. 2d, the eye activity can be identified as an eyeblink combined with a vertical movement. Note that this separation of different types of eye movement cannot be observed in the individual data channels. It illustrates the power of the multiple source modelling method to distinguish overlapping processes which are identified by their different topographies.

Note that the scaling in Fig. 2 was chosen to illustrate identification of eye activity. The ability of the method to remove the eye artifacts is comparable to traditional methods, as is shown below and by Lins et al. (1993).

(III) Comparisons between correction methods using human data

Comparison of methods is made on averaged epochs to auditory stimuli, containing either as few artifacts as possible, or containing large eye artifacts. In the data containing few artifacts it should be possible to observe distortions to EEG topography which result from correction. The data containing artifacts allow a comparison of the methods in their ability to remove the artifacts. Dipole modelling was used as a test that is sensitive to distortions in topography.

The MSEC method was applied using 3 ocular source components, and both optimizing and surrogate models of the EEG. It was compared to a traditional method, that of Elbert et al. (1985), which was selected for its use of the same number of components (EOG channels).

Scherg et al. (1989) were able to distinguish 3 dipolar sources in each temporal lobe that were able to account for the auditory N100 and sustained potential components of the ERP. In the current analysis, a simplified version of their analysis was used in which no attempt was made to differentiate sources within the temporal lobes, covering the interval surrounding the N100 peak (60–200 msec post stimulus). A regional source in each hemisphere was modelled that best fitted the data over the given time range, and we determined the orientation of this source at the maximum of the N100. Two points should be made about this approach: First, although the model is relatively simple, it describes the Scherg et al. data set reasonably well during the given time interval. On their data set (an average over 10 subjects) a residual variance of 0.5% was obtained over the time range 60–200 msec, using the equivalent analysis. Second, the steps involved in generating the simplified model are entirely mechanical, and therefore objective, and can be applied to individual subject (i.e., relatively noisy) data, even when there is heavy contamination from artifacts. The obtained sources should be similarly located as the Scherg et al. data set. Source orientations and locations will also depend on individual anatomy.

Method

Eight subjects aged between 26 and 40 were tested in an oddball paradigm. Stimuli were low-pass (2000 Hz) filtered noise bursts of 40 msec duration and 80 dB SPL, presented binaurally with interstimulus intervals varying randomly between 1.3 and 1.9 sec. Two types of rare stimulus consisted of the same noise bursts as the frequent stimuli, with the left or the right ear delayed by 1 msec compared with the other ear. The probability of occurrence of each type of rare stimulus was 0.125, and that for frequent stimuli was 0.75. Subjects were instructed to respond with a button press when the stimulus occurred in a specified ear. In alternating blocks, the left or the right ear was specified. Four blocks of 256 (192 frequent) stimuli were presented. During the last two blocks subjects were instructed to watch a central fixation point. No such instructions were given during the first two blocks. In 7 of the 8 subjects, this resulted in a large number of eye artifact epochs in blocks 1 and 2, and a relatively small number in the third and fourth block.

Between the second and third blocks, the subjects were required to perform calibration eye movements. They were asked to move their eyes horizontally at intervals of about 2 sec between two points 50 cm in front of them, separated by approximately 30° (± 15° to either side of a central fixation point). After 30 sec, they were asked to perform similar vertical movements. After another 30 sec, subjects were asked to look at the fixation point and blink once every approx. 2 sec for 30 sec.

Recording procedure

The EEG was recorded from 33 positions on the scalp and around the eyes. Positions were Fp1, Fp2, F7, F3, Fz, F4, F8, A1, A2 (mastoids), T3, C3, Cz, C4, T4, Cb1, T5, P3, Pz, P4, T6, Cb2, O1, O2, intermediate positions F3-Cz, F4-Cz, P3-Cz, P4-Cz, F7-C3, F8-C4, below each eye, left of the left eye, and right of the right eye. Cz was used as the common reference. An earth electrode was affixed to the forehead. A 32-channel DC amplifier (MES, Munich) recorded and digitized (16-bit, 5 bins/μV) the data continuously at 300 Hz with a low-pass filter setting of 70 Hz. Sintered Ag/AgCl electrodes, made by ZAK (Simbach), were attached using Grass EC2 electrode paste. Impedances were all below 5 kΩ. Each block of continuous DC-recorded data (approx. 7 min duration) was corrected for electrode drifts by spline subtraction (Bötzel et al. 1993).

Preparation of eye artifact correction coefficients

The calibration data were converted into 2000 msec epochs surrounding (1000 msec before to 1000 msec after) the onset of each eye movement or the maximum of each eye blink. The data were low-pass filtered at 8 Hz (24 dB/octave) and converted to average reference.

(1) Traditional method. A method based on that of Elbert et al. (1985) was used. Vertical, horizontal and radial EOG channels were computed as follows:
Horizontal channel: left of left eye − right of right eye (normal horizontal EOG).
Vertical channel: ((Fp1 + Fp2) − (below left eye + below right eye))/2 (mean of left and right vertical EOG).
Radial channel: ((Fp1 + Fp2 + below left eye + below right eye + left of left eye + right of right eye)/6 − (A1 + A2)/2) (mean of all electrodes near the eyes relative to mastoids).

Using a linear regression between the 3 EOG channels and each other channel, transmission coefficients were computed over all epochs of the calibration data.

(2) MSEC method. For the grand mean data, to allow the closest possible comparison between the methods, the coefficients generated by regression for the traditional method were used as source vectors. These were averaged over all 6 subjects included in the grand mean. For individual subjects, the first 3 PCA components (which explained approximately 95% of the data variance) were used, as described in Section I.

ERP data processing

Epoch classification. The data were converted to epochs ranging from 200 msec before to 1000 msec after each stimulus, low-pass filtered at 8 Hz (24 dB/octave) and converted to average reference. For the purpose of the present study, only responses to the frequent stimuli were investigated. Epochs were then viewed in the time range − 100 to + 300 msec relative to the stimulus and classified as "artifact-free," "containing eye artifacts" and "containing other artifacts." The third category included signals containing movement artifacts and large amplitude alpha. For subject 1, as will be further outlined below, systematic eye movements remained in the "artifact-free" averages, despite several increasingly conservative attempts at classification. In the following we shall continue to refer to the first category as "*artifact-free,*" retaining the quotes to stress the fact that not all artifacts were removed. We shall refer to the "containing eye artifacts" category as the *artifact* data.

Averaging. From each data set, a second traditionally corrected data set was generated by subtracting proportions of the vertical, horizontal and radial EOG from the data of each channel. Each data set was then averaged, separately for the "artifact-free" and for the artifact epochs. The averages contained between 68 and 654 epochs, except for one case of 20 artifact epochs for subject 2. Excluding the latter case, the mean number of epochs was 411 for "artifact-free" and

140 for artifact averages. The averages were baseline corrected by subtracting the mean of the time interval 20 msec before to 20 msec after stimulus onset from the data on each channel. Grand means of the traditionally corrected and the uncorrected data were generated over 6 subjects, excluding subjects 1 and 2.

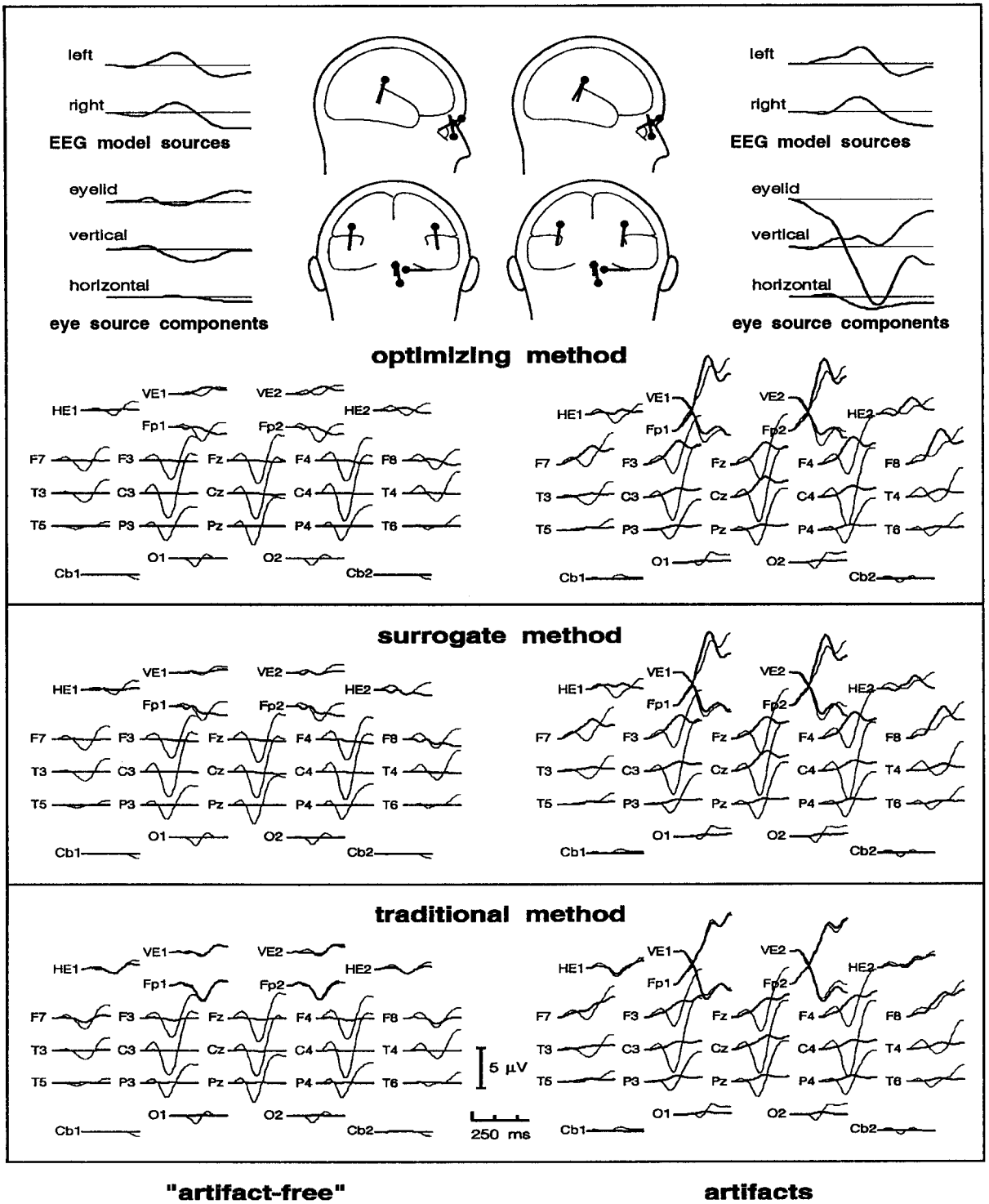

Fig. 3. Thin lines show grand means, using left mastoid reference, of the uncorrected "artifact-free" (left) and artifact (right) data. Thick lines show the signals that were subtracted in order to generate the corrected data for each method. Note the tendency of the traditional method to remove everything, including signals clearly due to brain activity (the N100) from channels near the eyes. The top of the figure shows source wave forms, locations and orientations for the optimizing MSEC method. The EEG sources are only shown for the component of the regional source which models the EEG activity best at the peak of the N100 at 120 msec. The eye source components indicate that there is eye activity in the "artifact-free" data.

Dipole source modelling. MSEC correction was performed on the averaged uncorrected data using the optimizing and the surrogate methods. The same initial model (Fig. 1a) as with the optimizing method was fitted to the uncorrected "artifact-free" and traditionally and surrogate corrected data over the time range 60–200 msec after the stimulus. With the optimizing method, no additional fitting was performed, because model fitting is integral to the method.

Seven sets of models were thus generated for each subject: uncorrected, traditional, surrogate and optimized correction for the "artifact-free" data, and traditional, surrogate and optimized correction for the artifact data. For each model, the residual variance and

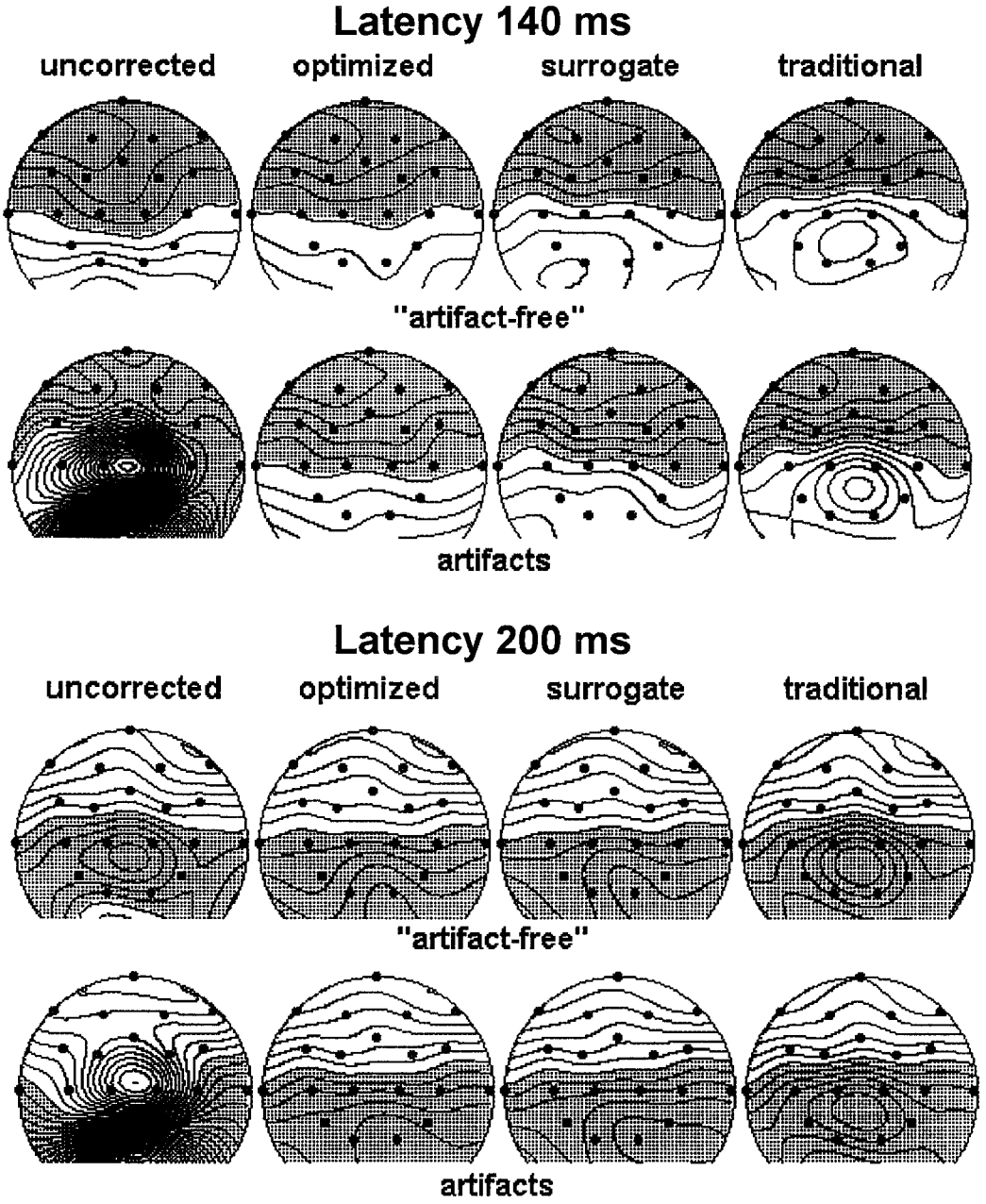

Fig. 4. Frontal view maps (projecting to 90° from centre point Fpz) of the grand mean average referenced data at latencies (a) 140 msec, where the difference between traditional and uncorrected data was largest, and (b) 200 msec, where the difference between optimized and uncorrected data was largest. Contour lines are separated by 0.5 μV. Negative regions are hatched. Dots show electrode locations. The 6 electrodes nearest the eyes are at the lower centre of the maps. The traditional method leads to circular contours around the eye electrodes, indicating that the method tends to equalize the potentials at these electrodes. At 140 msec the optimized MSEC method produced the most similar maps to the uncorrected ("artifact-free") data for both data sets. The circular contours at 200 msec on the uncorrected, "artifact-free" data are probably due to eye artifacts.

the location of the regional sources were recorded for comparison between the uncorrected and corrected data. In the grand mean, the orientation of each regional source at the maximum of the N100 peak measured at Cz was determined. In order to examine the effects of EOG electrode exclusion, a part of the above analyses was repeated without EOG electrodes.

Results

Analyses on the grand means

Averages and correction wave forms. The lower part of Fig. 3 shows the grand means of the uncorrected data for a subset of the data channels (thin lines), together with the signals that were subtracted in order to generate artifact corrected signals for each method (thick lines). The signals are all displayed referred to the left mastoid. As expected, the correction signals are largest at the eye and frontal electrodes and fall off towards the back of the head. The most important result is best observed in the "artifact-free" data. Here, the uncorrected data at eye electrodes clearly contain signals from the auditory ERP. For the traditional correction, correction signals at eye electrodes are almost identical to the uncorrected data, i.e., the method removes almost all the signals from these electrodes, including the N100 components. In the "artifact-free" data, the MSEC correction signals do not correlate highly with the uncorrected data. This indicates that, in contrast to the traditional method, the MSEC method is able to separate the contributions of brain and eye activity. Differences between the methods are still apparent in Fig. 3 at the other frontal electrodes, but are not visible at central and posterior electrodes. Finally, the MSEC method removed some signal from the "artifact-free" data. This appears to consist of a systematic eye movement artifact that increases towards longer latencies.

In the artifact data the larger part of the correction signals for all methods is clearly due to eye activity. Nevertheless, the tendency for the traditional method to remove everything including brain activity from eye electrodes is apparent.

Overlapping source wave forms. To illustrate how the MSEC method works, the top of Fig. 3 illustrates the separation of brain and eye activity in the optimizing method. For the brain activity, the source wave form of 1 of the 3 components of the left and right regional sources is shown. This is the component with the largest amplitude at the maximum of the N100, 120 msec after stimulus onset. The head diagrams show the location and orientation of this component. Centres of gravity of the eye source components, selected to identify eye activity, are represented as dipole sources near the eyes. The source wave forms of the eye source components illustrate that eye activity, in particular vertical and eyelid movement, is present in the "artifact-free" data set. In the artifact data set, the eye source wave forms are concentrated in the eyelid components, consistent with systematic eyeblinks, together with some vertical eye movements. The EEG source wave forms of the artifact data show similar activity to that of the "artifact-free" data. Differences between the wave forms and differences in location and orientation of the sources may be due to imperfect removal of the eye artifacts from the artifact data or to other noise in the data.

Data maps. It is instructive to examine the latencies at which the correction procedure has altered the data the most. In the "artifact-free" data, the largest differences between corrected and uncorrected wave forms are at Fp1 and Fp2. Fig. 4 shows frontal view spherical spline (Perrin et al. 1989) maps of the data at two latencies. At both latencies, the uncorrected artifact maps show large amplitude eye artifacts. At 140 msec (Fig. 4, top), traditionally corrected and uncorrected "artifact-free" data differ the most. In the traditionally corrected data, circular contours are apparent at eye electrodes which are not visible in the other corrected data and in the uncorrected "artifact-free" data. At 200 msec (Fig. 4, bottom), where the optimizing method differs the most from the uncorrected "artifact-free" data, the circular contours are also present in the traditionally corrected maps. Here the uncorrected "artifact-free" data also show circular contours, although these are shifted slightly upwards in comparison to the traditional maps. These contours are a further indication that the "artifact-free" data retain systematic eye artifacts.

An additional feature of the maps of the MSEC corrected data is the smooth horizontal contours (relative to the traditionally corrected data). This is consistent with the explanation that the eye artifacts have been removed without distorting the EEG topography.

Locations and orientations of the sources. Fig. 5 shows a comparison of the models fitted to the corrected and uncorrected data. As in Fig. 3, the orientation of the regional source at 120 msec after stimulus onset is shown. For both "artifact-free" and artifact data the source location after traditional correction is further forward and inward than after MSEC correction. For "artifact-free" data, location and orientation after MSEC corrections are closer to the uncorrected data model than the traditional model. For the uncorrected artifact data, the model is dominated by the eye activity and fitting locates the regional sources near the eyes.

Analyses on individual subject data

Residual variances. Table 1 shows the residual variances (RV) of the models before and after each type of

correction, for each subject and for the grand mean. RV is shown both *including* (top) and *excluding* (bottom) EOG electrodes.

The top of Table I shows two interesting features. First, the uncorrected "artifact-free" RV values are all higher than for the optimizing correction. In particular, subject 1 has an extremely large value of 34.3%. Examination of these data shows eye artifacts retained in the averages. Apparently there were small but systematic eye movements that were hardly visible in the raw data. The higher residual variances in the other subjects suggest the same, although to a lesser extent. Without EOG channels the differences were present, but smaller, in 7 of the 8 subjects (Table I, bottom). Thus the model deviates from the uncorrected data most at the EOG electrodes. Similarly, when modelling the grand mean of the uncorrected "artifact-free" data, the fit was poorest over the 4 channels above and below the eyes (RV $> 15\%$). Consistent with the other analyses on the grand mean data, these results all indicate the presence of eye artifacts in the "artifact-free" data.

Second, RV increases over the optimizing, surrogate and traditional correction methods for every subject, both for the "artifact-free" and artifact corrected data sets. Thus, by the criterion that a low residual variance indicates a better correction method, the two MSEC methods are clearly superior to the traditional method. These effects are statistically significant (1-tailed Sign test, $N = 8$, $P = 0.004$). When EOG electrodes are omitted, the differences among the methods are smaller, but RV is still lower in the optimizing and surrogate methods than in the traditional method in all except one comparison (subject 7, "artifact-free").

Source locations. As we have shown above, because of the eye artifacts in the "artifact-free" data, the model on the uncorrected data can be assumed to be more accurate when EOG electrodes are omitted. This model was therefore used as the reference against which the effects of correction on location were measured. Table II shows the distances from the reference location for the models after correction, and also for the uncorrected data set including EOG electrodes. For both MSEC methods, the distances were smaller

TABLE I

Residual variance (%) after fitting the model shown in Fig. 1a in the time range 60–200 msec compared between correction methods. Low values show good agreement between the model and the data. Means and standard deviations do not include subjects 1 and 2. The bottom line shows the results of fitting the grand mean data (excluding subjects 1 and 2).

Subject	Artifact-free	"Artifact-free"			Corrected artifacts		
		Optimizing	Surrogate	Traditional	Optimizing	Surrogate	Traditional
With EOG channels							
1	34.30	4.28	5.13	8.01	17.70	16.60	21.20
2	6.30	3.36	4.29	7.25	5.86	9.29	21.60
3	3.15	1.83	2.34	5.53	3.75	4.80	5.91
4	8.86	6.48	10.60	11.40	6.46	7.42	12.10
5	8.24	3.93	4.79	11.50	4.10	4.64	14.20
6	9.24	2.33	3.91	4.53	4.68	5.02	6.94
7	5.19	3.08	3.59	4.65	8.51	8.59	14.90
8	4.89	2.90	4.65	8.12	3.50	3.82	7.42
Mean	6.60	3.43	4.98	7.62	5.17	5.72	10.25
S.D.	2.51	1.66	2.89	3.24	1.95	1.86	3.96
Fits on means	7.09	3.42	5.44	6.76	3.19	3.94	6.94
Without EOG channels							
1	5.34	4.09	4.69	5.37	5.86	5.87	6.32
2	4.11	3.68	3.93	4.63	5.07	5.32	11.50
3	1.92	1.83	1.80	2.31	2.80	3.48	4.12
4	6.84	6.47	6.93	8.76	6.39	6.63	7.68
5	4.88	4.98	5.06	7.57	4.68	5.05	8.20
6	2.78	2.34	3.25	3.74	4.65	5.03	5.83
7	2.79	2.56	2.44	2.43	4.33	4.08	4.28
8	2.99	2.85	2.66	3.12	2.91	2.58	3.06
Mean	3.70	3.51	3.69	4.66	4.29	4.48	5.53
S.D.	1.82	1.81	1.94	2.79	1.33	1.42	2.07
Fits on means	4.05	3.57	4.52	4.79	3.27	3.66	4.26

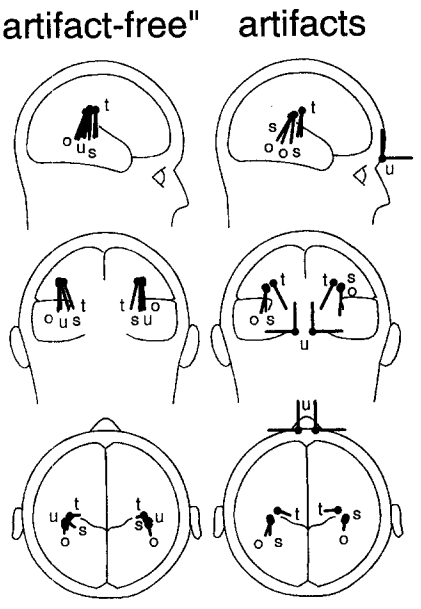

Fig. 5. Comparison of the models fitted to the uncorrected (u) and corrected (t = traditional; s = surrogate; o = optimized) grand mean data. The source locations are shown, together with the orientation at 120 msec after stimulus onset, where the N100 component had the largest amplitude at Cz. For the uncorrected artifact data, most of the data are dominated by eye activity and the sources are located near the eyes. Otherwise, for both the "artifact-free" and the artifact data the model after traditional correction locates more medially and anteriorly than those after source component correction methods. MSEC methods alter the model less than traditional correction.

than for the traditional method in every subject. When EOG electrodes were included, locations after optimizing correction were nearer to the reference data (mean = 2.5 mm, excluding subject 1) than were the uncorrected data (4.7 mm). For the surrogate method the mean distance was larger (8.6 mm), but still well below the mean for the traditional method (18.6 mm). If it is accepted that the data of subject 1 contain eye artifacts, the pattern of results is consistent across all subjects.

The results are similar after modelling without EOG electrodes (Table II, right), although the magnitude of the deviation is much smaller. This illustrates that the advantage of the MSEC method is retained, but is less dramatic, when EOG electrodes are omitted.

Discussion

Two main hypotheses were posed. One was that the traditional type of correction method distorts the EEG topography in a realistic data set. The other was that the MSEC method is able to provide a better correction, avoiding distortion of the EEG. Both hypotheses were confirmed.

The residual variance and location deviances showed clear superiority of the MSEC method over the traditional method for both the artifact and "artifact-free" data sets. The main disadvantage of the traditional approach is its tendency to remove the whole signal (including brain activity) from frontal and EOG electrodes (Figs. 3 and 4). The result of this distortion to topography on the models was to alter both the location and orientation of the dipole sources, as clearly seen in the corrected artifact data (Fig. 5, right).

An interesting finding was the presence of eye artifacts in the "artifact-free" data. The evidence of eye signals in the wave forms (Fig. 3) and the maps (Fig. 4) of the grand means, together with the higher residual variances (Table I) for the uncorrected data models, suggest that the MSEC locations were more reliable than those of the uncorrected data. Some eye artifacts contaminated the data in most, if not all subjects. The important message of this finding is that visual inspection or automatic methods to eliminate epochs contain-

TABLE II

Changes in location (in mm) of the model sources on corrected "artifact-free" data, compared to the model on uncorrected data without EOG electrodes, for each subject and for the mean over subjects 2–8 in the "artifact-free" data, including (left) and excluding (right) EOG electrodes. With the exception of subject 1 (without EOG), the MSEC methods resulted in smaller shifts in location than the traditional method. Since the uncorrected "artifact-free" data of subject 1 contained eye artifacts, the source locations after MSEC methods probably constitute the more accurate result.

Subject	With EOG channels				Without EOG channels		
	Uncorrected	Optimizing	Surrogate	Traditional	Optimizing	Surrogate	Traditional
1	20.2	8.5	12.0	20.7	8.4	8.0	4.8
2	5.9	1.8	4.1	14.0	1.8	1.2	4.6
3	4.4	1.1	0.6	15.3	1.1	1.4	5.0
4	9.3	7.8	11.5	24.9	2.3	3.3	6.6
5	4.5	1.7	7.3	8.4	1.7	1.4	3.9
6	1.0	3.5	5.0	7.7	3.5	2.3	4.8
7	3.4	1.2	11.0	29.4	1.2	3.1	6.9
8	4.6	0.5	20.7	30.7	0.5	4.3	6.8
Mean	4.7	2.5	8.6	18.6	1.7	2.4	5.5

ing eye artifacts in the raw data are likely to leave a certain amount of eye activity in the uncorrected averages. This can have a large effect on modelling results, especially when information from frontal electrodes is important.

The effect of eye artifacts on the uncorrected "artifact-free" data was largest at the EOG electrodes. Therefore the uncorrected "artifact-free" data without EOG electrodes were used to generate the reference model. With EOG electrodes included, modelling after using the optimizing MSEC method produced the most similar source localizations to the reference model. Using the surrogate method produced localizations that were less accurate, but well below the deviations resulting from traditional correction. When EOG electrodes were omitted, the relationships among the methods were retained, but the deviations were smaller. These results suggest the following conclusions about the use of correction methods and frontal electrodes. First, if the optimizing MSEC method is used, frontal (including EOG) electrodes can be used for the analysis of brain activity, particularly in the frontal cortex. Second, in the absence of frontal brain processes, omission of EOG electrodes will lead to more accurate modelling results, irrespective of the correction method. Third, both MSEC methods are preferable to the traditional method, whether or not EOG electrodes are retained.

The surrogate method produced results intermediate between the optimizing MSEC and traditional methods. This indicates that the separation of overlapping brain and eye activity was less than optimal when using the surrogate model. On the other hand, this method has the advantage that prior knowledge of the sources underlying the EEG is not required. However, any prior knowledge of the sources of the EEG can be used to improve the surrogate method. For instance, in the case of the auditory N100, two regional sources in the vicinity of the temporal lobes should improve artifact correction, because most of the brain activity is located there. Our use of a surrogate model that did not match the sources of the N100 well demonstrates the feasibility of the MSEC method even if very little is known about the source locations.

One innovation of the MSEC method is its ability to separate overlapping EEG and eye activity. The other is its possible use to identify eye activity in both averaged and raw EEG data. The examples described in Section II (Fig. 2) showed how overlapping components of eye movements were distinguished in the identification wave forms in a way that single data channels cannot. This suggests a number of potential uses of the method, in which the surrogate method is used as a relatively automatic method for modelling the EEG. For example, an EEG display could show the artifact-corrected EEG together with eye activity channels. Another application could be the automatic identification of eye movements, which should be more reliable than methods based on pattern recognition in a single data channel, such as that of Gratton et al. (1983) for recognizing blinks, because the MSEC method integrates the information from all data channels.

Removal of the EEG present in the EOG is only one of a number of problems confronted by artifact treatment methods (Brunia et al. 1989). Two other factors to be discussed are the number of components used for eye correction (Möcks et al. 1989; Berg and Scherg 1991a, Lins et al. 1993) and the accuracy with which the components are estimated. These problems apply to both the MSEC and traditional methods and may be in part responsible for the differences in results between artifact and "artifact-free" data. Our artifact data included many epochs with eye movements larger than those of the calibration. In this situation artifact correction is likely to perform sub-optimally (Berg and Scherg 1991a).

Another problem is the question whether transmission of eye activity to EEG electrodes might change between calibration and the recording of the remaining data. Unless only blink artifacts are to be corrected, we do not see an alternative to using calibration data, because the eye movements in the measurement data seldom produce enough variance to estimate the source vectors or transmission coefficients with sufficient accuracy. Judging by the results of source modelling (Berg and Scherg 1991a), the main source of changes between calibration and recording is probably a change in the position of the eyes relative to the head. For example, this can occur if the subject is sitting upright during calibration and lying down during measurements.

More accurate eye movement calibration could have removed a larger number of ocular source components, particularly from the artifact data set. On the other hand the eye movements included in the artifact averages were much larger than in most data sets and therefore, the correction procedure applied here may represent a practical procedure in most situations. The use of a central fixation point could help to improve the calibration (Lins et al. 1993). This sets a baseline from which to compute the amplitudes of each eye movement. Artifact treatment could also be improved by excluding eye movements larger than those occurring during calibration.

The MSEC method makes use of the topographic information at all electrodes to estimate the eye activity. It could be argued that EOG electrodes are therefore no longer necessary, because information about eye activity is present everywhere on the head. However, the more electrodes near the eyes that are included, the more accurate the modelling of eye activity will be. Some improvement may be achieved by includ-

ing the nasion and electrodes immediately above the eyes. Furthermore, the exact positioning of electrodes relative to the eyes is less important than in the traditional bipolar recordings of the vertical and horizontal EOG. Because of the procedure with which source vectors are computed, the head model is optimally adjusted to the given electrode locations for the EOG. It is nevertheless important to measure electrode locations accurately, in order to model the brain activity more precisely. EOG as well as EEG should be recorded using a common reference, to treat the data from all electrodes equivalently.

As an artifact treatment method, the optimizing MSEC method is most suitable in the context of source modelling. Models can be developed on uncorrected data, using the ocular source components to account for the eye activity. The surrogate method can be used more widely. It will be less effective than the optimizing method because, by definition, the EEG modelling is only approximate. However, we have shown that it is superior to the traditional methods in its effects on EEG topography, and in addition, it provides a separate display of each type of eye movement. As computing power increases and topographic analyses become more sophisticated, the ability of the MSEC method to resolve EEG and eye activity will become increasingly important.

This study was supported by a grant from the McDonnell-Pew Foundation (Grant 90-174, principal investigator Edgar Zurif).

We are indebted to Jutta Keppner for her assistance with data collection, and to Dan Ruchkin and Michael Wagner for useful comments and suggestions.

References

Achim, A., Richer, F. and Saint-Hilaire, J.-M. Methods for separating temporally overlapping sources of neuroelectric data. Brain Topogr., 1988, 1: 22–28.

Baumgartner, C., Sutherling, W.W., Shi, D. and Barth, D.S. Investigation of multiple simultaneously active brain sources in the electroencephalogram. J. Neurosci. Meth., 1989, 30: 175–184.

Berg, P. and Scherg, M. Modelling the ocular dipoles. In: C.H.M. Brunia, A.W.K. Gaillard and A. Kok (Eds.), Psychophysiological Brain Research, Vol. 1. Tilburg University Press, Tilburg, 1990: 22–25.

Berg, P. and Scherg, M. Dipole models of eye movements and blinks. Electroenceph. clin. Neurophysiol., 1991a, 79: 36–44.

Berg, P. and Scherg, M. Dipole modelling of eye activity and its application to the removal of eye artifacts from the EEG and MEG. Clin. Phys. Physiol. Meas., 1991b, 12 (Suppl. A): 49–54.

Billings, R.J. The origin of the initial negative component of the averaged lambda potential recorded from midline electrodes. Electroenceph. clin. Neurophysiol., 1989, 72: 114–117.

Bötzel, K., Plendl, H., Paulus, W. and Scherg, M. Bereitschaftspotential: is there a contribution of the supplementary motor area? Electroenceph. clin. Neurophysiol., 1993, 89: 187–196.

Brunia, C.H.M., Möcks, J. and Van den Berg-Lennsen, M. Correcting ocular artifacts – a comparison of several methods. J. Psychophysiol., 1989, 3: 1–50.

De Munck, J.C., Van Dijk, B.W. and Spekreijse, H. Mathematical dipoles are adequate to describe realistic generators of human brain activity. IEEE Trans. Biomed. Eng., 1988, 35: 960–966.

Ebersole, J.S. EEG dipole modelling in complex partial epilepsy. Brain Topogr., 1991, 4: 113–123.

Elbert, T., Lutzenberger, W., Rockstroh, B. and Birbaumer, N. Removal of ocular artifacts from the EEG – a biophysical approach to the EOG. Electroenceph. clin. Neurophysiol., 1985, 60: 455–463.

Gratton, G., Coles, M.G.H. and Donchin, E. A new method for off-line removal of ocular artifact. Electroenceph. clin. Neurophysiol., 1983, 55: 468–484.

Lins, O., Picton, T.W., Berg, P. and Scherg, M. Ocular Artifacts in recording EEGs and event-related potentials. II. Source dipoles and source components. Brain Topogr., 1993, 6: 65–78.

Möcks, J., Gasser, T. and Sroka, L. Approaches to correcting EOG artifacts. In: C.H.M. Brunia, J. Möcks and M. Van den Berg-Lennsen (Eds.), Correcting Ocular Artifacts – a Comparison of Several Methods. J. Psychophysiol., 1989, 3: 21–26.

Perrin, F., Pernier, J., Bertrand, O. and Echallier, J.F. Spherical splines for scalp potential and current density mapping. Electroenceph. clin. Neurophysiol., 1989, 72: 184–187.

Scherg, M. Fundamentals of dipole source potential analysis. In: F. Grandori, M. Hoke and G.L. Romani (Eds.), Auditory Evoked Magnetic Fields and Electric Potentials. Advances in Audiology, Vol. 6. Karger, Basel, 1990: 40–69.

Scherg, M. and Picton, T.W. Separation and identification of event-related potential components by brain electric source analysis. In: C.H.M. Brunia, G. Mulder and M.N. Verbaten (Eds.), Event-Related Potentials of the Brain (EEG Suppl. 42). Elsevier, Amsterdam, 1991: 24–37.

Scherg, M. and Von Cramon, D. Topographical analysis of auditory evoked potentials: derivation of components. In: R.H. Nodar and C. Barber (Eds.), Evoked Potentials, II. Butterworth, Woburn, 1984: 73–81.

Scherg, M. and Von Cramon, D. Two bilateral sources of the late AEP as identified by a spatio-temporal dipole model. Electroenceph. clin. Neurophysiol., 1985, 62: 32–44.

Scherg, M. and Von Cramon, D. Evoked dipole source potentials of the human auditory cortex. Electroenceph. clin. Neurophysiol., 1986, 65: 344–360.

Scherg, M., Vajsar, J.J. and Picton, T.W. A source analysis of the human auditory evoked potentials. J. Cogn. Neurosci., 1989, 1: 336–355.